CAMES, **28**(1): 39–55, 2021, doi: 10.24423/cames.284

Structural Design Optimization of Steel Beams and Frames with Web-Tapered Members Using the PSO-FEM Algorithm

Piotr SYCH, Marek SŁOŃSKI*

Computational Engineering, Faculty of Civil Engineering
Cracow University of Technology
Warszawska 24, 31-155 Kraków, Poland
*Corresponding Author e-mail: marek.slonski@pk.edu.pl

This paper presents an algorithm for structural design optimization of steel beams and frames with web-tapered members using the particle swarm optimization (PSO) algorithm and the finite element method (FEM). The design optimization is done in accordance with Eurocode 3 (EC 3) for the minimum mass. The proposed algorithm is more flexible and efficient than traditional design methods based on a trial and error approach. The effectiveness of the presented PSO-FEM algorithm is evaluated on examples of the size optimization of web-tapered members cross-section. The results show that the PSO-FEM algorithm is feasible and effective for finding useful designs.

Keywords: structural design optimization, particle swarm optimization, finite element method, web-tapered members.

1. Introduction

In recent years, steel beams and frames with web-tapered members have attracted more and more interest [1–4]. This is due to their better distribution of internal forces throughout structural members and more economical material usage in comparison to regular frames.

To successfully design a portal frame with web-tapered members, it is often necessary to simultaneously find several geometrical parameters. The web-tapered member design requires the selection of member section sizes. The searching for the optimal designs for these types of sections is rather a complex task because of the large number of design variables, and the selection is typically performed through trial and error [5].

The design problem is nonlinear, which may cause difficulties for gradient-based optimization methods. Currently, structural design optimization of steel

beams and frames with tapered members using population-based algorithms is of significant research interest. In [6], Kaveh and Ghafari compared nine metaheuristics in the design optimization problem for steel frames with tapered members. Hasançebi *et al.*, in [7], compared non-deterministic search techniques in the optimum design of real-size steel frames. The applications of PSO for structural design optimization were also considered in [1, 8, 9].

Structural design optimization is a process of finding the optimal structure, and it may lead to substantial savings. This process covers topology optimization, shape optimization and/or size optimization [10]. In comparison to the common design process where the shape of the structure, the cross-sections, boundary conditions and materials are known in advance, and the deformation and the internal forces are computed, the structural optimization design process is a kind of an inverse problem. During the design process, we usually obtain a structure in which the stress ratio (capacity ratio) is not optimally distributed. It is often the case that in one cross-section, the structure is under-stressed, and in another cross-section, the structure is over-stressed. As a result, the design process requires several steps to obtain a satisfactory solution, which is typically far from the optimal one. In the case of large and complicated structures this design process can be very time-consuming.

The description of optimization problems is given in [11], where linear programming was applied for optimization of frames and trusses. Design computations were based on the limit states method, which led to nonlinear constraints. As shown in [11], structural design optimization problems, due to nonlinear constraints, cannot be solved using the direct application of linear programming. In that case, we have to turn to the approximate methods.

Metaheuristic methods, for example PSO [12, 13], can be applied to problems with linear and nonlinear cost functions and constraints. The sole disadvantage of the metaheuristic methods is the fact that these methods lead to good solutions but not the best ones. We often do not have certainty that the best solution exists and can be found [14].

This solution is acceptable because we obtain a better structure than a structure designed by trial and error. Especially in the case of steel structures, due to the high cost of the material, application of structural optimization and obtaining a few percent lighter structure can be useful.

This paper presents an algorithm for the optimized designs of non-prismatic steel I-section members based on minimum mass, taking into account applied forces and limit states such as maximum displacement. The process begins with the definition of an objective function and the constraints. The objective function is usually defined as the total mass of the structure.

This paper is organized as follows. In Sec. 2, the description of the PSO-FEM algorithm is presented. Section 3 presents three examples of design optimization

problems: Gerber beam, double-span beam and portal frame. In Sec. 4 short discussion of results is given and in Sec. 5 final conclusions are presented.

2. PSO-FEM algorithm for EC 3-based design optimization

Steel portal frames are designed according to one of several design methods. For example, Eurocode 3: Design of steel structures (EN 1993) – EC 3 describes how to design steel structures, using the limit state design philosophy [15]. The design of steel portal frames with tapered members is a complex task that requires some approximations to be made [16]. In this paper, EN 1993 interaction formulae are applied. While this method is more conservative than others, it is the most computationally effective [17].

In this paper, we consider a structural design optimization problem as a size optimization problem. The design variables are the dimensions of a cross-section of an I-shaped steel member, such as the height of the web and the thickness of the flange. The objective is the minimum of the total mass of the structure. We assume the following constraints in the form of limit states:

1) From ultimate limit state (ULS):

$$\frac{N_{Ed}}{N_{c,Rd}} + \frac{M_{Ed}}{M_{c,Rd}} \leq S_R, \tag{1}$$

where N_{Ed} – the design value of the compression force, $N_{c,Rd}$ – the design cross-sectional resistance of the sections to uniform compression force, M_{Ed} – the design bending moment, $M_{c,Rd}$ – the design cross-sectional bending moment resistance, S_R – the stress ratio (set to two values: 0.9 or 0.8).

2) From serviceability limit state (SLS):

$$w \leq w_{\max}, \tag{2}$$

where w – deflection, $w_{\max}$ – maximum deflection ($L/250$ for beams and frames and $L/200$ for purlins), L – span.

PSO is a population-based stochastic algorithm for solving continuous and discrete optimization problems. The PSO algorithm is a kind of nature-inspired metaheuristics and was first proposed by Kennedy and Eberhart in [12]. It solves optimization problems by using a set of candidate solutions (particles) known as a population. These particles are moved around in the search-space according to a few simple mathematical formulae describing updating of the particle position and velocity.

The updated position vector $\mathbf{x}_i$ of each particle at iteration i is computed as:

$$\mathbf{x}_i = \mathbf{x}_{i-1} + \mathbf{v}_i \Delta t, \tag{3}$$

where Δt is the time step value (in this paper, a fixed value $\Delta t = 1$ is assumed) and $\mathbf{v}_i$ is the corresponding updated velocity vector defined as:

$$\mathbf{v}_i = \omega \mathbf{v}_{i-1} + \mathbf{v}_c + \mathbf{v}_s, \tag{4}$$

where ω is the inertia weight, $\mathbf{v}_c$ is the cognitive part of the velocity and $\mathbf{v}_s$ is the social part of the velocity. The updated velocity vector $\mathbf{v}_i$ of each particle at iteration i is computed as:

$$\mathbf{v}_i = \omega \mathbf{v}_{i-1} + c_1 r_1 \frac{\mathbf{p} - \mathbf{x}_{i-1}}{\Delta t} + c_2 r_2 \frac{\mathbf{g} - \mathbf{x}_{i-1}}{\Delta t}, \tag{5}$$

where $\mathbf{v}_{i-1}$ is the velocity vector at iteration $i-1$, r_1 and r_2 are random numbers between 0 and 1; $\mathbf{p}$ represents the best ever particle position for each particle and $\mathbf{g}$ represents the global best position in the swarm up to the iteration i. The parameter c_1 is a cognitive parameter and the parameter c_2 is a social parameter in the PSO nomenclature.

The basic steps of the PSO algorithm are as follows:

1) Initialize particles' positions randomly distributed in the design space and their velocities.
2) Compute the value of the objective function for each particle.
3) Update the optimum particle position and global optimum particle position.
4) Update the position of each particle using its previous position and updated velocity vector.
5) Repeat steps 2–4 until the stopping criteria are met.

Finite element method (FEM) is the most widely used computational method for solving various engineering problems described by partial differential equations (PDEs) [18, 19]. FEM is also widely applied for computing structure deformations, internal forces and stresses. Finite element analysis (FEA) is thus a key element of the engineering design of structures.

In the PSO-FEM algorithm, the design objective is formulated as an objective function. PSO is applied for searching the optimal values of design variables by minimizing the objective function in the space of feasible solutions. The FEM solver, in which the design variables are used as input variables, provides results that allow to check the fulfillment of constraints in the form of limit states. Then, the global search for the optimal solution is converted to finding the best particle.

When the PSO-FEM algorithm is started, positions and velocities of particles are randomly initialized with respect to assumed constraints. Then, in each iteration, the particles are assigned to structure parameters and the FEM solver is applied for computing maximal stress ratio and maximal deflection. If the

newly generated particles lead to FEM solutions that do not satisfy (1) or (2), they are not taken into account during updating the personal best position and the global best position and they do not influence the optimization.

Next, the personal best position and the global best position are updated according to the value of the objective function computed for each particle. Finally, velocities and positions are updated according to Eqs (5) and (3), respectively. The described above updating algorithm is repeated until specified stopping criteria are met. In Fig. 1, a flowchart of the PSO-FEM algorithm is presented.

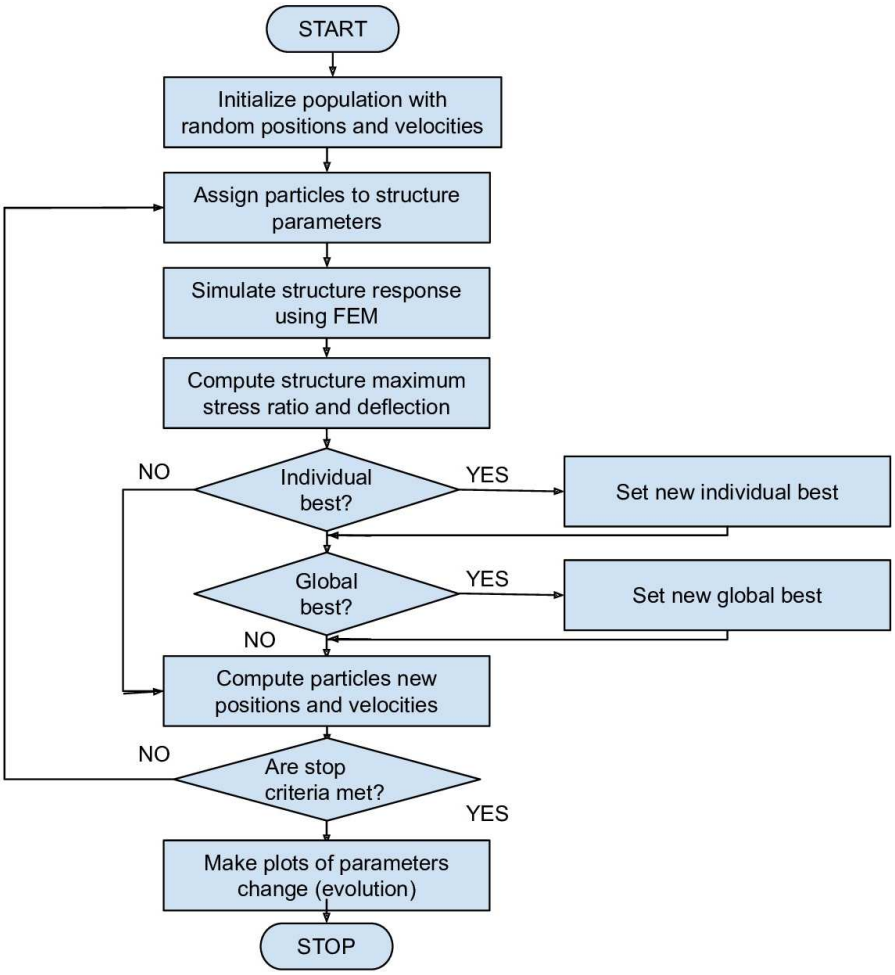

Fig. 1. Flowchart of the PSO-FEM algorithm for EC 3-based design optimization.

In numerical examples presented below, the structural design of beams and frames is done according to EC 3 [15]. For computing structure displacements

and internal forces, we use in-house software based on FEM for bar structures. This software was written in C++ and run under Linux OS. It combines internally FEM and PSO algorithms, which allows efficient data transfer during the PSO-FEM based optimization process. The problem of repeatability of results is solved by setting the seed of a pseudorandom numbers generator (PRNG) to a known value.

3. Examples of structural design optimization

3.1. Gerber beam

In this section, we illustrate the workflow presented in the previous section by applying the PSO-FEM algorithm to the optimization of a Gerber beam with three spans and two hinges. The beam is assumed to be symmetrical. Such beams are often used as purlins in industrial halls. The schematic diagram of the beam is shown in Fig. 2, together with its geometrical and statical parameters. Figure 3 presents a schematic diagram of a three-beam structure corresponding to beam in Fig. 2. The beam is made of a steel IPE 180 cross-section (Class 1) and has a span with a length assumed to be 5850 mm. The beam is loaded with a design constant loading 40 kN/m.

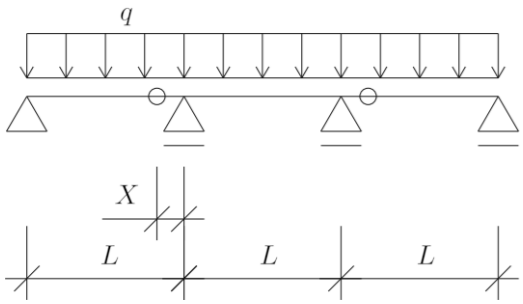

Fig. 2. Schematic diagram of a Gerber beam with two hinges (depicted by small circles).

Fig. 3. Schematic diagram of a three-beam structure corresponding to beam in Fig. 2.

The design variable X for this simple optimization problem is the distance from the support to the hinge, see Fig. 2. The goal of the analysis is to find such a value of variable X for which the maximum bending moment in the end-span

is equal to the absolute value of the maximum bending moment at the support, and as a result, the stress ratio for the whole beam would be minimal.

3.1.1. Analytical solution. In the analytical solution, the maximum bending moment M_{span} for a simply supported beam with the $L - X$ span length is

$$M_{\text{span}} = q(L - X)^2/8, \tag{6}$$

and the reaction force R is

$$R = q(L - X)/2. \tag{7}$$

The maximum bending moment at the support M_{sup} is

$$M_{\text{sup}} = RX + qX^2/2. \tag{8}$$

By equating Eqs (6) and (8), after some modifications, we finally obtain a quadratic equation with respect to X

$$X^2 - 6LX + L^2 = 0. \tag{9}$$

The analytical solution of the optimization problem is the positive root of the quadratic equation shown in Eq. (9). For example, for $L = 5850$ mm we obtain an analytical solution $X = 1003.7$ mm.

3.1.2. Numerical PSO-FEM based design solution. The objective function in this example is defined as the maximum value of the stress ratio $\dfrac{M_{Ed}}{M_{c,Rd}}$, where M_{Ed} is the design bending moment and $M_{c,Rd}$ is the design cross-sectional bending moment resistance (see Eq. 6.12 in EC 3 for Section Class 1, [15]).

The assumed constraints are: for the ultimate limit state (ULS) the assumed stress ratio is below 0.9 and for serviceability limit state (SLS) we assume $w <= w_{\max} = L/200$ (for purlins according to EC 3). The statical analysis is carried out by using an analytical formula for the maximal bending moment and the maximal deflection of the simply supported beam (instead of FEM).

In numerical experiments, we assume the design variable domain for parameter X to be 400 mm $\leq X \leq$ 1541 mm, from which we sample the initial parameter value X_i for each particle. After 10 iterations of the PSO algorithm, we obtained the solution $X = 1004.7$ mm for the span length $L = 5850$ mm, which is very close to the analytical solution $X = 1003.7$ mm. Similarly, for the span length $L = 7000$ mm, the PSO-based solution was close to $X = 1189$ mm, which is also very close to the analytical solution $X = 1201$ mm.

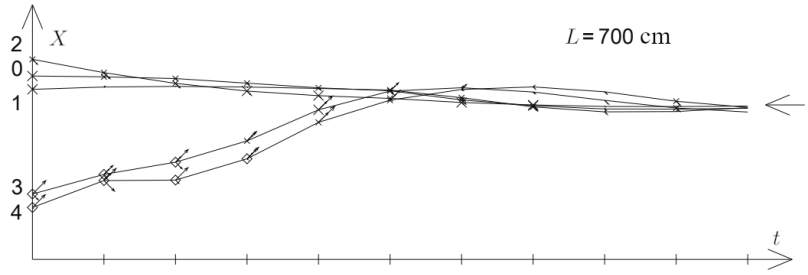

Fig. 4. Plot of optimization process of X parameter for the Gerber beam using five particles (horizontal arrow indicates analytical solution).

In Fig. 4, a plot of the optimization process of X parameter for the Gerber beam is presented, for a beam with the span length $L = 7000$ mm, applying only five particles. The horizontal arrow on the right side of the plot indicates the analytical solution. As can be seen all particles converged to the analytical solution ($X = 1003.7$ mm).

3.2. Double-span beam

The subject of the second optimization example was a web-tapered simply supported two-span beam with the span length L and the column height h. The span was 2×25 m and the level difference between the ridge and the outer supports was 2.5 m. A schematic diagram of the beam is shown in Fig. 5. The beam is made of steel (S355) as a welded plate girder with an I-beam cross-section. The web height over the outer supports was assumed to be H_1 and the flange thickness was assumed to be t_{f_1}. Over the middle support, the web height H_2 and the flange thickness t_{f_2} were assumed. In the beginning, it was assumed that the beam width was 330 mm and the web thickness was 10 mm.

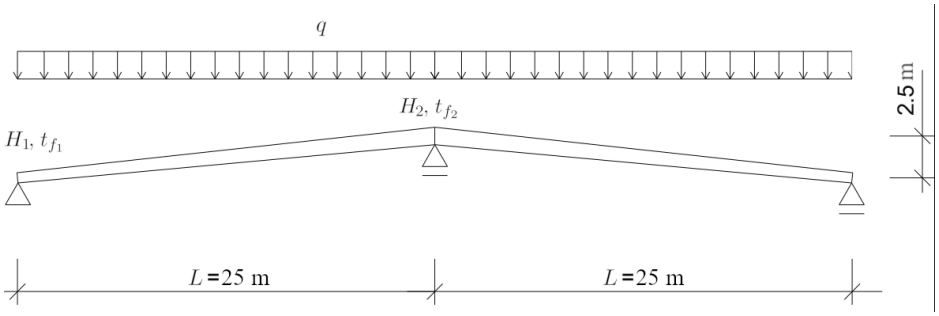

Fig. 5. Schematic diagram of the web-tapered two-span beam with its geometrical parameters.

During the FEM-based analysis, the beam was divided into eight finite elements with constant cross-section. In the design process, the asymmetrical snow

loading condition was taken into account. The best velocities presented in Subsec. 3.3 were applied in the PSO algorithm.

The optimization problem for the beam with tapered members is formulated below:

$$\text{Minimize} \quad f_w(\overline{x}), \tag{10}$$

$$\text{Subject to} \quad g_{\text{SLS}}(\overline{x}) \geq 0, \tag{11}$$

$$g_{\text{ULS}}(\overline{x}) \geq 0, \tag{12}$$

$$\overline{x} \in \{x_1 = H_1, x_2 = t_{f_1}, x_3 = H_2, x_4 = t_{f_2}\}, \tag{13}$$

where f_w is the objective function, g_{SLS} refers to the SLS constraint and g_{ULS} refers to the ULS constraint.

In this experiment, $f_w(\overline{x})$ refers to the objective function describing the search for the minimum mass of the beam. The solutions are checked against constraints in Eqs (11) and (12). Each design variable has its own range of values coming from design restrictions and parts available in production.

The results of numerical experiments for a various number of particles and 60 iterations are presented in Table 1. The best solution was obtained for the fifth experiment with 100 particles: $H_1 = 668$ mm, $t_{f_1} = 11$ mm, $H_2 = 966$ mm, $t_{f_2} = 19$ mm. The maximal deflection was, in that case, 87 mm. The results show that the mass of the best solution in each experiment depends on the number of particles and probably also on c_1 and c_2.

Table 1. Geometrical parameters of the web-tapered steel beam for a various number of particles N after 60 iterations T of the PSO-FEM algorithm.

Experiment	N	T	H_1 [mm]	t_{f1} [mm]	H_2 [mm]	t_{f2} [mm]	Mass [kg]
1	5	60	603	13	1019	19	7393
2	10	60	609	13	1027	19	7378
3	20	60	618	13	1033	19	7358
4	50	60	605	13	1038	19	7357
5	100	60	**668**	**11**	**966**	**19**	**7287**
6	200	60	616	13	1024	19	7365

3.3. Portal frame

In this example, we consider a web-tapered portal frame with I-shaped doubly symmetric cross-sections made of steel (S355) welded plates. The main advantage of the welded plates is that their dimensions can be easily fitted to the project

requirements, which is not the case for the prismatic members with fixed cross sections. Figure 6 shows a schematic diagram of the portal frame.

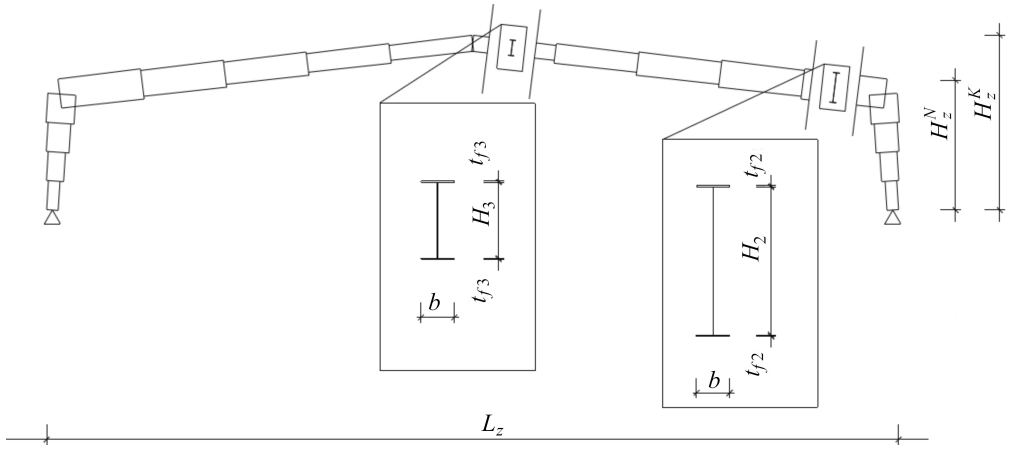

Fig. 6. Schematic diagram of the web-tapered portal frame with its geometrical parameters.

We analyze frames with assumed outer dimensions. It means that we have to compute the position of the central axis of the frame in consecutive iterations according to the change of height of the rafters and the change of thickness of the flanges. The outer dimensions of the frame are set as:

- L_z – span of the frame (71 800 mm),
- H_z^K – height of the frame, from the base to the top (14 800 mm),
- H_z^N – height of the frame, from the base to the connection (10 860 mm).

The width of the column and the rafter are assumed to be 560 mm. The following geometrical parameters are being optimized:

- H_2 – height of the rafter at the connection,
- H_3 – height of the rafter at the top,
- t_{f2} – flange thickness of the rafter at the connection,
- t_{f3} – flange thickness of the rafter at the top.

The FEM model with several finite elements with fixed cross-sections is used in place of a model with rafters and columns with variable cross-sections. It is assumed that the flanges thickness and rafters height are changing linearly along the length of the element. Calculations of internal forces are carried out based on the FEM model consisting of 18 elements and 19 nodes. It is assumed that the frame is simply supported. To simplify the task, concentrated loads from purlins are replaced by an evenly distributed load. It is assumed that the frame is concentrated by densely spaced purlins so that the effect of lateral-torsional buckling is ignored in the calculations. In the structural design optimization, it

is assumed that the stress ratio (S_R) calculated according to Eq. (1) at no point in the frame could exceed 0.8.

In numerical experiments, the normalization of frame parameters and velocities was applied and initially population of nine particles was assumed. Parameter values were initiated with pseudo-random values ranging from 0.5 to 1.0 for H_2, t_{f2} and t_{f3}. The parameter H_3 was initiated in the range from 0 to 0.5. The velocity values were initialized from -1.0 to 1.0.

The optimization problem for the frame with tapered members is formulated below:

$$\text{Minimize} \quad f_w(\overline{x}), \tag{14}$$

$$\text{Subject to} \quad g_{\text{SLS}}(\overline{x}) \geq 0, \tag{15}$$

$$g_{\text{ULS}}(\overline{x}) \geq 0, \tag{16}$$

$$\overline{x} \in \{x_1 = H_2, x_2 = t_{f_2}, x_3 = H_3, x_4 = t_{f_3}\}, \tag{17}$$

where f_w is the objective function, g_{SLS} refers to the SLS constraint and g_{ULS} refers to the ULS constraint. In this experiment, $f_w(\overline{x})$ refers to the objective function describing the search for the minimum mass of the beam. The solutions are checked against constraints in Eqs (15) and (16). Each design variable has its own range of values coming from design restrictions and parts available in production.

3.4. Results of numerical experiments

Below we present the results of five numerical experiments for the structural design optimization of the portal frame with web-tapered members with five different settings for the PSO-FEM algorithm. The final dimensions of the cross-sections are also collected in Table 2.

3.4.1. Optimization with only nine particles. During experiments, it was found that using only nine particles that satisfy the constraints leads to fast convergence but the result for one particle was inaccurate. Figure 7 shows the initial problem with convergence for this particle during optimization of the parameter H_2. Therefore, the parameter t_{f3} for particle number 7 was initialized in a different range (from 0 to 0.5) so that the particle did not satisfy the constraints at the beginning of the optimization process. Finally, the optimal parameters found by the PSO-FEM algorithm, after 14 iterations, were:

- $H_2 = 1795$ mm,
- $H_3 = 1198$ mm,

- $t_{f2} = 39$ mm,
- $t_{f3} = 25$ mm,
- mass = 29 636 kg.

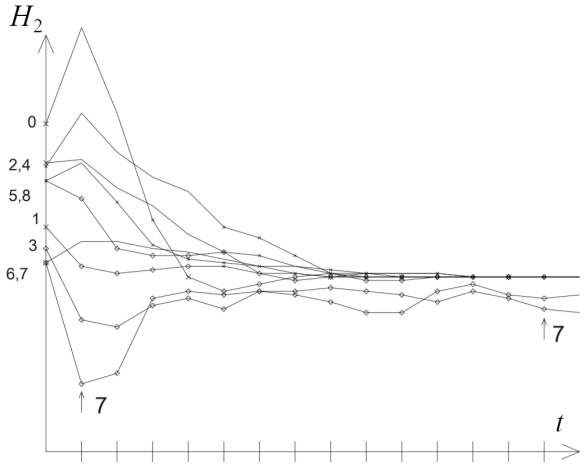

FIG. 7. Plot of changes of the parameter H_2 with pointed particle number 7.

The value of flange thickness ($t_{f2} = 39$ mm) obtained as a result of the calculations is considered to be too large.

3.4.2. Optimization for different ways of computing cognitive component of velocity. In Fig. 7, bad convergence of particles number 3 and 7 may be seen. The reason for this is the way of computing the cognitive component of velocity $\mathbf{v}_c$ (described in Eq. (5)) for particles, which in previous iterations did not satisfy the assumed constraints. This velocity was calculated on the basis of $\mathbf{p}$ ("personal best value" from Eq. (5)), which is incorrect for these particles.

It is worth noting that optimized parameters are cross-section dimensions. This statement indicates that if the constraints are not satisfied, then the parameters are too small. Then, it is recommended to use the positive value of $\mathbf{v}_c$. In further calculations, for particles that in previous iterations did not satisfy the constraints and elements of $\mathbf{v}_c$ that were less than zero were set to zero. This way, the obtained velocity of particles should be positive due to the remaining components of their velocity.

Despite the apparent faster convergence, the calculated parameter values changed very little: $H_2 = 1793$ mm, $t_{f2} = 39$ mm, $H_3 = 1208$ mm, $t_{f3} = 25$ mm, mass = 29 536 kg. It was assumed that the convergence runs too fast and only at first 10 iterations $\mathbf{v}_c = 0$ was set, which did not significantly improve the result. Figure 8 shows the plot of optimization of the parameter H_2 for the frame assuming $\mathbf{v}_c = 0$. It is worth emphasizing that the results are still far

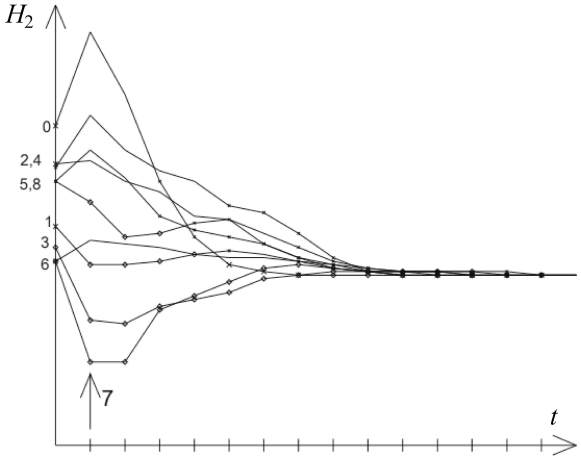

FIG. 8. Plot of changes of the parameter H_2 assuming $\mathbf{v}_c = 0$.

from optimal ones, even though the parameters, values visible in Fig. 8 seem to change towards the optimal value.

3.4.3. Optimization with a large number of particles. The number of particles was increased from 9 to 50, which still did not significantly improve the results: $H_2 = 2546$ mm, $t_{f2} = 30$ mm, $H_3 = 870$ mm, $t_{f3} = 24$ mm, mass $= 28\,982$ kg. The results are presented in Fig. 9.

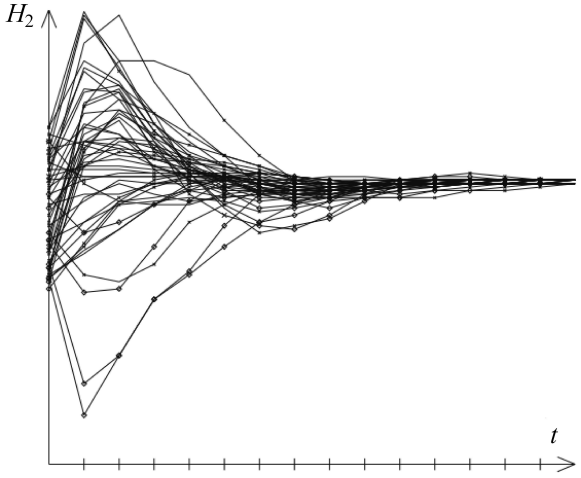

FIG. 9. Plot of changes of the parameter H_2 using 50 particles.

3.4.4. Optimization with variable parameter ω. According to [20], a variable parameter value ω (described in Eq. (4)) was applied. The convergence of the

solution was lost for ω greater than 0.4. Therefore, the linear reduction of the parameter ω has been applied during iteration from value 0.4 to 0.1. After 15 iterations, the results were obtained: $H_2 = 2467$ mm, $t_{f2} = 33$ mm, $H_3 = 848$ mm, $t_{f3} = 25$ mm, mass =30 366 kg, which means that parameter variability did not improve the optimization in our case.

3.4.5. Optimization using velocities of the best particles. In order to improve the optimization, the velocity of the best particles was remembered for use in the next iterations. The "best particles" were considered the ones that satisfied the constraints and ensured the largest decrease in the optimization function. That signifies the highest value of the velocity gradient. It is important to note that even better results were obtained using pseudorandom numbers as velocities when the rate of iteration decreased.

In the current experiment, 25 particles were applied. From the first to the nineteenth iterations, the particles with the highest value of the velocity gradient were selected and memorized. After 20 iterations, the particles, velocity assumed pseudorandom values from 0.0 to 1.0 (first vertical arrow in Fig. 10). After 40 iterations, the particles, velocities were assigned the best-remembered velocities from previous iterations. This place is marked in Fig. 10 with the second vertical arrow.

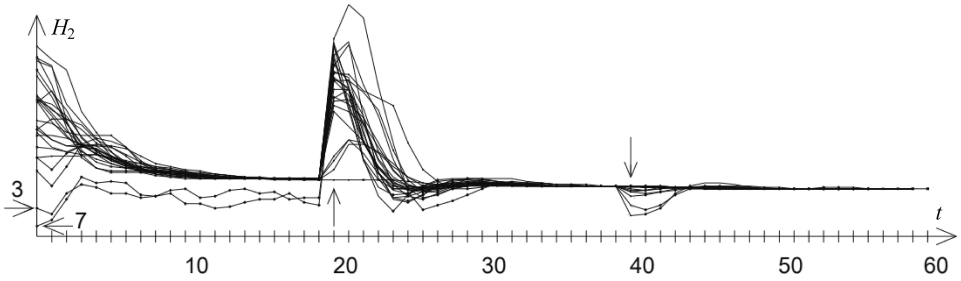

FIG. 10. Plot of changes of H_2 using velocities from "the best particles" and pseudorandom.

After 60 iterations, the following results were obtained: $H_2 = 2313$ mm, $t_{f2} = 25$ mm, $H_3 = 1079$ mm, $t_{f3} = 20$ mm, mass = 26 550 kg. As a result of the optimization, the parameters of the construction with minimum mass and low thickness of the plates were finally obtained.

Table 2 presents the summary of the results, where N depicts the total number of particles used in the structural design optimization and T is the total number of iterations of the PSO-FEM algorithm. As can be seen, the best solution (experiment 5) is about 10% better than the worst optimal solution (experiment 4).

Table 2. Geometrical parameters of the web-tapered steel portal frame for a various number of particles N and iterations T of the PSO-FEM algorithm.

Experiment	N	T	H_2 [mm]	t_{f2} [mm]	H_3 [mm]	t_{f3} [mm]	Mass [kg]
1	9	14	1795	39	1198	25	29 636
2	9	14	1793	39	1208	25	29 536
3	50	14	2546	30	870	24	28 982
4	50	15	2467	33	848	25	30 366
5	25	60	**2313**	**25**	**1079**	**20**	**26 550**

4. Discussion

During the optimization process, it is important to maintain the diversity of particles, including ones that initially do not fulfill the optimization requirements. This deliberate treatment allows to obtain better results.

In the case of the optimization of structures with a number of parameters greater than one, it is usually not possible to obtain the optimal results globally. In this case, for the normalization of the design parameters, more particles and more iterations are usually needed. Moreover, to avoid local minima it can be useful to assign to velocities pseudorandom values saved as the best in initial iterations.

It was experimentally stated that the best optimization results are obtained for the parameters c_1 and c_2 in the interval from 0.3 to 0.5. The parameter ω should be not greater than 0.4. For greater values of the parameter ω, the optimization process is divergent. Changing ω during the optimization process did not have a positive impact on the results.

5. Final conclusions

In this paper, we have shown that the PSO-FEM algorithm is able to optimize a steel structure: both a simple one such as a Gerber beam and more complicated structures such as a two-way beam and a portal frame. For the Gerber beam, the obtained solution is close to the exact (analytical) solution. We have applied PSO with only 5 particles and only 10 iterations were needed. For the portal frame, we have applied PSO with 25 particles and 60 iterations. Moreover, some improvements to the basic PSO algorithm were needed. For the two-way beam and the portal frame, the obtained solutions are close to the solutions obtained by a simple "trial and error" method but probably better due to the uniform stress ratio along the length of the structure. For the Gerber beam, the obtained solution has equal bending moments in the outer span and in the support.

The application of the PSO-FEM algorithm-based optimization process also allows to assess the direction of structure parameters' change during the design process made by hand. For example, it is possible to objectively assess which changes are better. Also, more parameter combinations can be checked in a shorter time.

The welded plate girder obtained during the optimization process has a mass probably close to the optimal one but also fulfills the optimization requirements in all cross-sections: not exceeding stress ratio and ultimate deflection. This approach allows to obtain the most important parameters of the optimized structure quicker than by using the "trial and error" method. This optimized structure also carries out the applied loading safely.

In this work, we have investigated to some extent the effects of random values of PSO parameters on the results of design optimization with the PSO-FEM algorithm, and we have found that the effects are rather negligible. In future work, we plan to investigate these effects in more detail because this can be beneficial to estimate the uncertainty in the obtained solutions.

Acknowledgments

The first author would like to thank Prof. Zenon Waszczyszyn for fruitful discussions and help during the preparation of the first version of this paper.

References

1. H. Aucamp, The optimisation of web-tapered portal frame buildings, Master's thesis, Stellenbosch University, Republic of South Africa, 2017, https://scholar.sun.ac.za/bitstream/handle/10019.1/101099/aucamp_optmisation_2017.pdf?sequence=1.

2. P. Hradil, M. Mielonen, L. Fülöp, Optimization tools for steel portal frames-effective modelling of lateral supports, *Research report VTT-R-00567-11*, VTT Technical Research Centre of Finland, Espoo, 2011.

3. R.C. Kaehler, D.W. White, Y.D. Kim, *Frame design using web-tapered members*, American Institute of Steel Construction, 2011.

4. L. Marques, L.S. da Silva, C. Rebelo, A. Santiago, Extension of EC3-1-1 interaction formulae for the stability verification of tapered beam-columns, *Journal of Constructional Steel Research*, **100**: 122–135, 2014.

5. W.Y. Jeong, Structural analysis and optimized design of general nonprismatic I-section members, Ph.D. thesis, Georgia Institute of Technology, USA, 2014.

6. A. Kaveh, M.H. Ghafari, Geometry and sizing optimization of steel pitched roof frames with tapered members using nine metaheuristics, *Iranian Journal of Science and Technology, Transactions of Civil Engineering*, **43**(1): 1–8, 2019.

7. O. Hasançebi, S. Çarbaş, E. Doğan, F. Erdal, M.P. Saka, Comparison of non-deterministic search techniques in the optimum design of real size steel frames, *Computers & Structures*, **88**(17–18): 1033–1048, 2010.

8. R.E. Perez, K. Behdinan, Particle swarm approach for structural design optimization, *Computers & Structures*, **85**(19–20): 1579–1588, 2007, https://www.sciencedirect.com/science/article/abs/pii/S0045794907000399.

9. M.G. Sahab, V.V. Toropov, A.H. Gandomi, A review on traditional and modern structural optimization: problems and techniques, [in:] A.H. Gandomi, X.-S. Yang, S. Talatahari, A.H. Alavi [Eds], *Metaheuristic Applications in Structures and Infrastructures*, pp. 25–47, Elsevier, 2013, https://www.sciencedirect.com/science/article/pii/B9780123983640000024.

10. P. Christensen, A. Klarbring, *An introduction to structural optimization*, Springer Science & Business Media, 2009, https://link.springer.com/book/10.1007/978-1-4020-8666-3.

11. M. Kleiber (ed.), *Handbook of computational solid mechanics: survey and comparison of contemporary methods*, Springer, Berlin, Heidelberg, 1998, https://books.google.pl/books?id=YVvJMAEACAAJ.

12. J. Kennedy, R. Eberhart, Particle swarm optimization, [in:] *Proceedings of ICNN'95 – International Conference on Neural Networks*, Perth, Australia, Vol. 4, pp. 1942–1948, IEEE, 1995, https://ieeexplore.ieee.org/document/488968.

13. D. Wang, D. Tan, L. Liu, Particle swarm optimization algorithm: an overview, *Soft Computing*, **22**(2): 387–408, 2018, https://link.springer.com/article/10.1007%2Fs00500-016-2474-6.

14. A.H. Gandomi, X.-S. Yang, S. Talatahari, A.H. Alavi, Metaheuristic algorithms in modeling and optimization, [in:] *Metaheuristic Applications in Structures and Infrastructures*, pp. 1–24, Elsevier, 2013, https://www.sciencedirect.com/science/article/pii/B9780123983640000012.

15. EN 1993, Eurocode 3: Design of steel structures, CEN, 2004.

16. M.P. Saka, Optimum design of steel frames with tapered members, *Computers & Structures*, **63**(4): 797–811, 1997.

17. P. Hradil, M. Mielonen, L. Fülöp, Advanced design and optimization of steel portal frames, *Journal of Structural Mechanics*, **43**(1): 44–60, 2010.

18. M.J. Turner, R.W. Clough, H.C. Martin, L.J. Topp, Stiffness and deflection analysis of complex structures, *Journal of the Aeronautical Sciences*, **23**(9): 805–823, 1956.

19. O. Zienkiewicz, *The finite element method*, 3rd ed., McGraw-Hill, New York, 1977.

20. F. Sahin, A. Devasia, Distributed particle swarm optimization for structural Bayesian network learning, [in:] F. Chan, M.K. Tiwari [Eds], *Swarm Intelligence, Focus on Ant and Particle Swarm Optimization*, pp. 532 IntechOpen, Vienna, Austria, 2007, https://www.intechopen.com/books/swarm_intelligence_focus_on_ant_and_particle_swarm_optimization/distributed_particle_swarm_optimization_for_structural_bayesian_network_learning.

Received February 18, 2020; revised version December 15, 2020.